Fluid and gyrokinetic modelling of particle transport in plasmas with hollow density profiles

Fluid and gyrokinetic modelling of particle transport in plasmas with hollow density profiles

Journal of Physics: Conference Series **775** (2016) 012014 doi:10.1088/1742-6596/775/1/012014

Fluid and gyrokinetic modelling of particle transport in plasmas with hollow density profiles

D Tegnered, M Oberparleiter, H Nordman and P Strand

Department of Earth and Space Sciences, Chalmers University of Technology, SE-412 96 Gothenburg, Sweden

E-mail: tegnered@chalmers.se

Abstract. Hollow density profiles occur in connection with pellet fuelling and L to H transitions. A positive density gradient could potentially stabilize the turbulence or change the relation between convective and diffusive fluxes, thereby reducing the turbulent transport of particles towards the center, making the fuelling scheme inefficient. In the present work, the particle transport driven by ITG/TE mode turbulence in regions of hollow density profiles is studied by fluid as well as gyrokinetic simulations. The fluid model used, an extended version of the Weiland transport model, Extended Drift Wave Model (EDWM), incorporates an arbitrary number of ion species in a multi-fluid description, and an extended wavelength spectrum. The fluid model, which is fast and hence suitable for use in predictive simulations, is compared to gyrokinetic simulations using the code GENE. Typical tokamak parameters are used based on the Cyclone Base Case. Parameter scans in key plasma parameters like plasma β, R/L_T, and magnetic shear are investigated. It is found that β in particular has a stabilizing effect in the negative R/L_n region, both nonlinear GENE and EDWM show a decrease in inward flux for negative R/L_n and a change of direction from inward to outward for positive R/L_n. This might have serious consequences for pellet fuelling of high β plasmas.

1. Introduction

The characteristics of particle transport in regions of hollow density profiles is an important issue for fusion plasmas. For example, reactor grade plasmas will likely be fuelled by pellet injection that will transiently perturb the density and temperature profiles, making the density profile hollow. A similar effect on the density profile may occur in connection with the L-mode to H-mode transition. Hence, it is important to study the microstability and transport properties in regions with a hollow density profile. In a microstability study of pellet fuelled discharges in MAST [1] using the local gyrokinetic code GS2 [2] in linear mode, a stabilization of all modes was found in the negative R/L_n region as a result of the reduction in η_i and η_e, as well as a high sensitivity to the rapid change in plasma β and collisionality that was caused by the pellet ablation. In [3] a stabilizing effect was also found for pellet fuelled discharges at JET. The linear growth rates as well as the nonlinear heat fluxes were shown to be reduced in the positive gradient region. The quasilinear gyrokinetic code QuaLiKiz [4] was used in [5] to study the microturbulence during the L to H transition, it was shown that the TE mode was stabilized and that the particle flux was highly sensitive to the sign of R/L_n as well as the collisionality and R/L_T.

In order to study the effects the positive density gradient ($R/L_n < 0$ where $R/L_n = -R\nabla n/n$)

Table 1: Typical CBC parameters

Parameter	Value
Collisions	No (unless noted)
β	No (unless noted)
q_0	1.4
$\hat{s}$	0.8
B_0	3.1 T
r/R	0.18
R	1.65 m
$T_e = T_i$	2.85 keV
$n_e = n_i$	$3.5 \times 10^{19}\,\mathrm{m}^{-3}$
$R/L_T = R/L_{T_i} = R/L_{T_e}$	6.96

and parametric scans have on the transport the gyrokinetic code GENE [6] is used in local mode to study the transport due to Ion Temperature Gradient (ITG)/Trapped Electron (TE) mode [7, 8, 9, 10, 11, 12, 13] turbulence. Parameter scans around those of the Cyclone Base Case (CBC) [14] are used. The CBC parameters are shown in Table 1. The linear and nonlinear GENE results are compared to results from a fluid model, an extended version of the Weiland [15] transport model, the Extended Drift Wave Model (EDWM) [16].

2. GENE and EDWM simulations setup

GENE solves the nonlinear gyrokinetic Vlasov equations together with Maxwell's equations in order to find the distribution functions of the species, $f\left(\mathbf{R}, v_\parallel, \mu, t\right)$, the electrostatic potential, $\phi(\mathbf{x}, t)$ and the parallel components of the magnetic vector potential and magnetic field, $A_\parallel(\mathbf{x}, t)$ and $B_\parallel(\mathbf{x}, t)$. It is a Eulerian δf-type code where the coordinate system is aligned to the background magnetic field with x as the radial coordinate, y as the binormal coordinate, and z as the parallel coordinate. Both linear and nonlinear simulations are performed with kinetic ions and electrons. In the collisional cases, the collisions are modelled using a linearised Landau-Boltzmann collision operator [17]. The pressure gradient, as used in the calculation of the curvature and ∇B drift, is set to be consistent with the density and temperature gradients and the plasma β. In this work, a circular geometry model is used. For the nonlinear GENE simulations, a simulation domain in the perpendicular plane of $[L_x, L_y] = [126, 126]$ is used, with a resolution of $[n_x, n_y] = [96, 48]$. In the parallel direction 32 grid points are used, and in the parallel velocity direction 64 grid points, and 16 magnetic moments. The simulations are typically run up to a simulation time of $t = 300R/c_s$ where R is the major radius and $c_s = \sqrt{T_e/m_i}$. The resolution and simulation domain are checked through convergence tests.

EDWM is an extended version of the Weiland [18, 15] model which incorporates an arbitrary number of ion species in a multi-fluid description and an extended wavelength spectrum. Here, the wavelengths are fixed at $k_y\rho_s = 0.2$, for the comparison to nonlinear GENE since it is the wavelength corresponding to the largest fluxes, or $k_y\rho_s = 0.3$ for the linear comparison since it is the wavelength corresponding to the largest ITG growth rates. ρ_s is the sound Larmor radius defined as $\rho_s = c_s/(eB/m_s c)$. In the fluid model, the perturbations in density, parallel velocity, and temperature for each species is described by the continuity, parallel momentum and energy equations, including FLR-effects for the main ions. The densities of the main ions, trapped, and free electrons are coupled through the quasineutrality condition. The free electrons are assumed

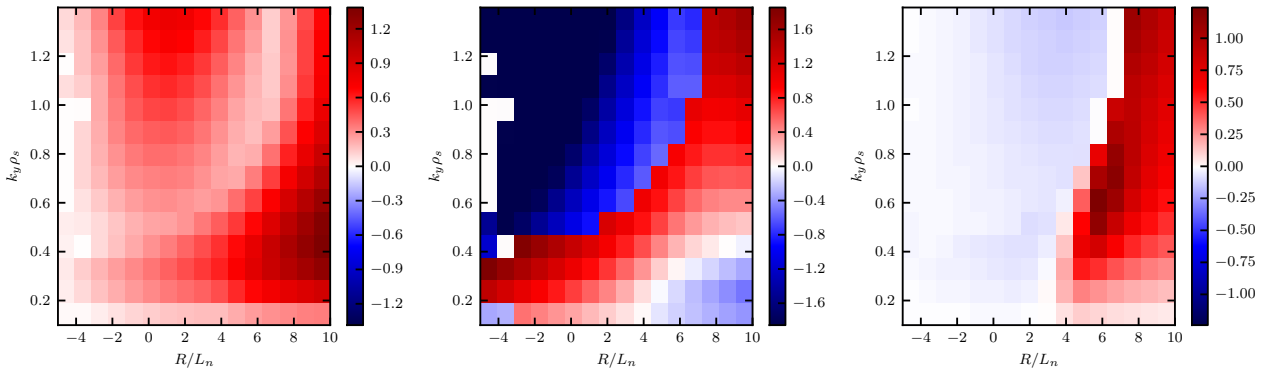

(a) Linear growth rate, γ (b) Linear real frequency, ω_r (c) Normalized flux, $\Gamma/\delta n^2$

Figure 1: GENE eigenvalues as a function of $k_y\rho_s$ and $R/L_{n_e} = R/L_{n_i}$ for the mixed case where $R/L_{T_e} = R/L_{T_i} = 6.96$.

to be Boltzmann distributed in the electrostatic case. A weakly ballooning eigenfunction is assumed whereby the parallel wavenumber $k_\parallel$, the perpendicular wavenumber $k_\perp$ and the magnetic drift ω_{Dj} can be replaced by averages over the weakly ballooning eigenfunction. The particle and heat fluxes are then calculated assuming linear relations between the field quantities combined with a modified mixing length estimate [15].

3. Linear results

The computational parameters used in the linear GENE simulations are a resolution of 48×12 in the parallel and normal direction with 32 grid points in the parallel velocity direction and 24 magnetic moments. An initial value solver is used. Three main cases are simulated linearly: the mixed case with $R/L_{T_e} = R/L_{T_i} = 6.96$, a case where the ITG mode is primarily unstable with $R/L_{T_e} = 0, R/L_{T_i} = 6.96$ and a case where the TE mode is primarily unstable with $R/L_{T_e} = 6.96, R/L_{T_i} = 0.0$.

In Figure 1 the linear growth rates, real frequencies and normalized particle fluxes $\Gamma/\delta n^2$ are shown for the mixed case as a function of the normalized density gradient scale length R/L_n and the normalized poloidal wave number $k_y\rho_s$. In the mixed case, the ITG mode is dominating roughly in the area $k_y\rho_s < 0.5$ and $R/L_n < 4$ and the area $k_y\rho_s > 0.5$ and $R/L_n > 6$ as indicated by the positive values of the real frequencies in Figure 1b. Here a positive ω_r means that the mode is drifting in ion diamagnetic direction, indicating an ITG mode. The TE mode is dominant elsewhere, as indicated by the negative real frequency. In Figure 1c the direction of the particle flux is indicated at different wave numbers and density gradients in the mixed case. Positive values correspond to an outward particle flux while negative correspond to an inward one. The gradient of zero particle flux, indicating the background peaking factor, increases with wave number from $PF \approx 3$ at $k_y\rho_s = 0.2$ to 6 at $k_y\rho_s = 1.2$.

Moving to the pure ITG case in Figure 2 the eigenvalues corresponding to the ITG mode are similar, but the spectra lacks the TE mode that was previously visible for lower R/L_n and higher wave numbers. There is no clear region with inward particle flux as in the mixed case.

Finally, in Figure 3 the eigenvalue spectra of the TE case is examined. Here, the TE mode dominates everywhere and is is stabilized at large negative R/L_n. There is a region of inward transport at large negative R/L_n which however coincides with low growth rates since the TE mode is stabilized in the negative R/L_n region.

In Figure 4 the eigenvalues of GENE and EDWM are compared in a scan in R/L_n. In the

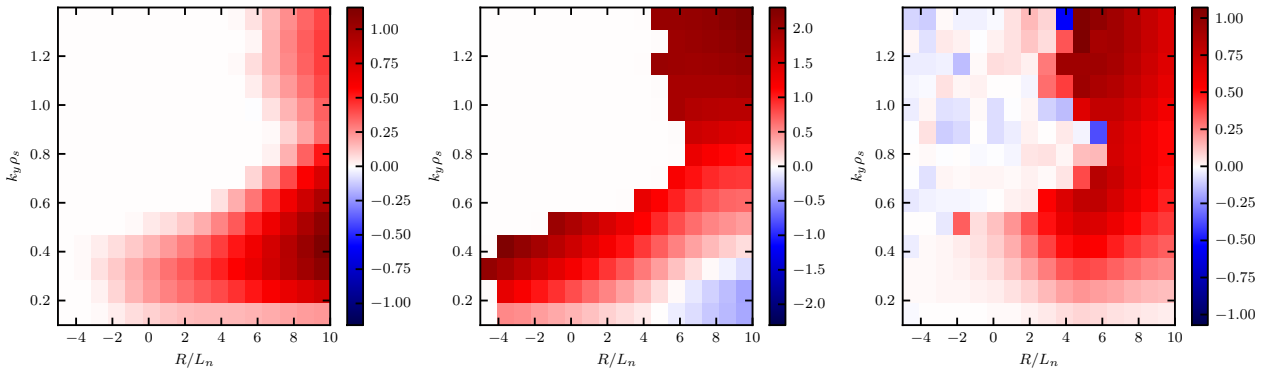

(a) Linear growth rate, γ (b) Linear real frequency, ω_r (c) Normalized flux, $\Gamma/\delta n^2$

Figure 2: GENE eigenvalues as a function of $k_y\rho_s$ and $R/L_{n_e} = R/L_{n_i}$ for the ITG case where $R/L_{T_e} = 0.0$, $R/L_{T_i} = 6.96$.

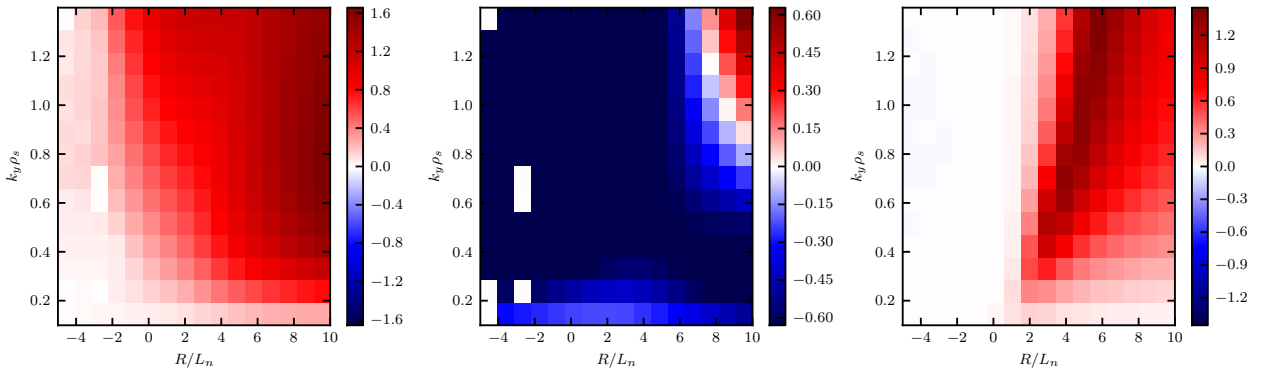

(a) Linear growth rate, γ (b) Linear real frequency, ω_r (c) Normalized flux, $\Gamma/\delta n^2$

Figure 3: GENE eigenvalues as a function of $k_y\rho_s$ and $R/L_{n_e} = R/L_{n_i}$ for the TE case where $R/L_{T_e} = 6.96$, $R/L_{T_i} = 0.0$.

mixed and ITG cases (Figures 4a and 4b) which are both ITG dominated at these wave numbers, the real frequencies match well while the growth rates are significantly reduced in GENE for lower and negative R/L_n. In the TE dominated case, Figure 4c, the growth rates are more similar while the gyrokinetic real frequencies are closer to 0. As an indication of the direction of the gyrokinetic and fluid particle fluxes, $\Gamma/(q_i + q_e)$, where q_i and q_e are the ion and electron heat fluxes, is also shown in Figure 4. Vertical lines indicate the lowest R/L_n where the particle flux changes sign. This matches well between the fluid and gyrokinetic models in the mixed case while in the TE case the R/L_n of zero particle flux is lower for the gyrokinetic model. No negative particle flux is found at this wave number for the pure ITG case.

Next, the dependence on plasma β is explored in Figure 5. β effects in GENE are included as magnetic field fluctuations parallel and perpendicular to the background field, however, since a concentric circular geometry model is used, there is no Shafranov shift. For negative R/L_n β is stabilizing in both models. The MHD ballooning limit can be estimated by $0.6\hat{s}/\left[q_0^2(2R/L_n + R/L_{T_i} + R/L_{T_e})\right]$ [19], so $\beta_{\text{crit,MHD}} = 1.8\%$ for $R/L_n = 0$ and $\beta_{\text{crit,MHD}} = 6.2\%$ at $R/L_n = -5$. Thus, for sufficiently large negative R/L_n, the Kinetic Ballooning Mode

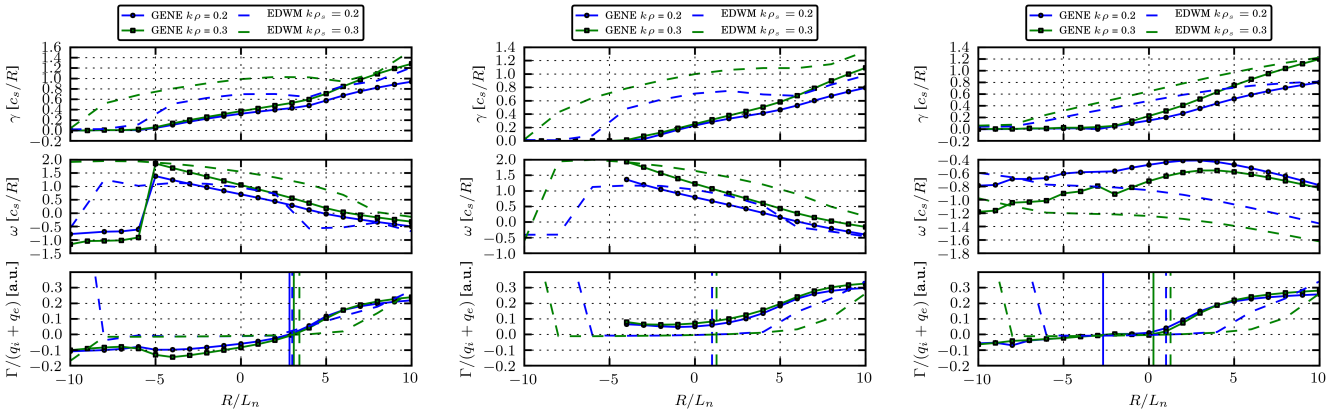

(a) The mixed ITG/TE case (R/L_{T_e} = $R/L_{T_i} = 6.96$)

(b) The pure ITG case ($R/L_{T_e} = 0$, $R/L_{T_i} = 6.96$)

(c) The pure TE case ($R/L_{T_e} = 6.96$, $R/L_{T_i} = 0$)

Figure 4: Comparison of linear gyrokinetic and fluid eigenvalues in scan over R/L_n. Normalized particle flux also shown. Vertical lines indicate value of R/L_n where the particle flux changes sign.

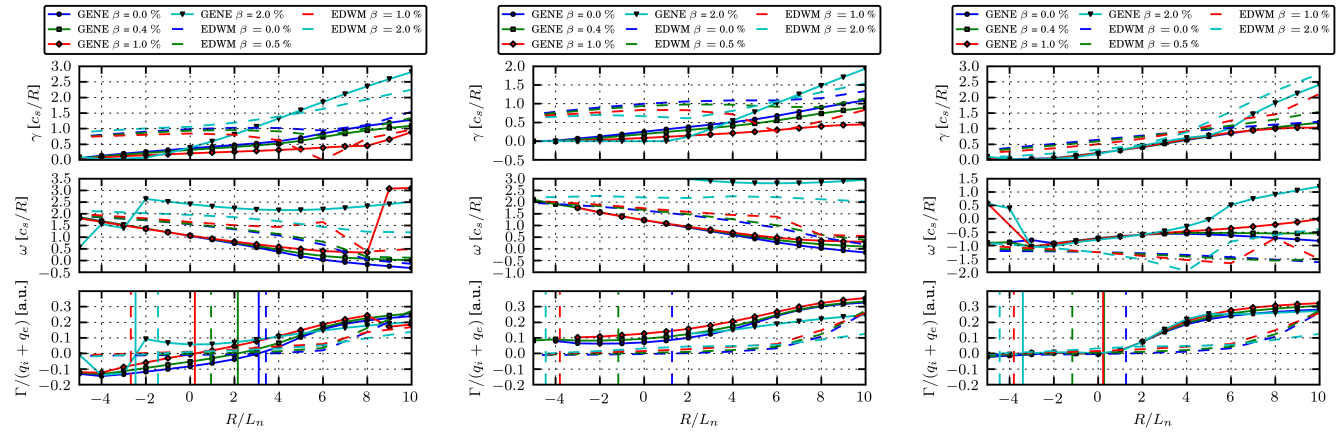

(a) The mixed ITG/TE case (R/L_{T_e} = $R/L_{T_i} = 6.96$)

(b) The pure ITG case ($R/L_{T_e} = 0$, $R/L_{T_i} = 6.96$)

(c) The pure TE case ($R/L_{T_e} = 6.96$, $R/L_{T_i} = 0$)

Figure 5: Linear gyrokinetic and fluid eigenvalues at $k_y\rho_s = 0.3$ in scan over R/L_n and plasma β. Normalized particle flux also shown. Vertical lines indicate value of R/L_n where the particle flux changes sign.

(KBM) will not be excited and the ITG mode will be dominant for which β has a stabilizing effect, which is consistantly found in gyrokinetic simulations [20]. Both models also show a decreasing peaking factor with increasing β in the ITG dominated cases in Figures 5a and 5b, consistent with earlier gyrokinetic findings [21].

In a scaling of collisionality in GENE without changing the temperature or density, it was found that higher collisionality did not stabilize the ITG or TE mode turbulence significantly in the negative R/L_n region. A reduction in the (still positive) background peaking factor was found, which is a known result [21]. A reduction in growth rates with higher magnetic shear in the positive and negative gradient region was found for the ITG and TE dominated cases, along with a reduction in the still positive background peaking factor.

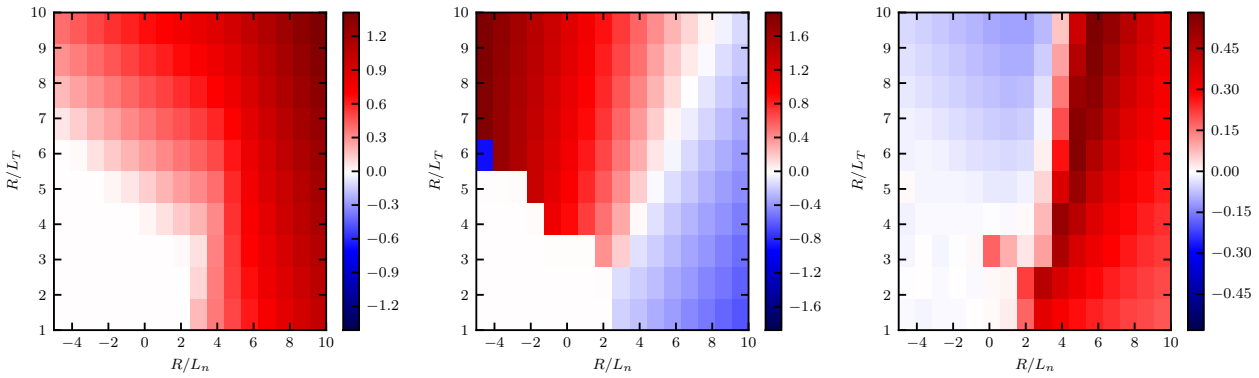

(a) Linear growth rate, γ (b) Linear real frequency, ω_r (c) Normalized flux, $\Gamma/\delta n^2$

Figure 6: GENE eigenvalues as a function of R/L_n and $R/L_{T_i} = R/L_{T_e}$ at $k\rho = 0.3$

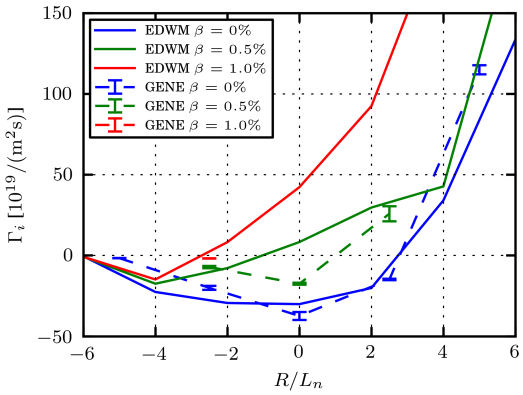

Figure 7: Nonlinear gyrokinetic particle flux as a function of R/L_n and plasma β, compared to EDWM results.

In order to study the turbulence closer to marginal stability, a scan in $R/L_T = R/L_{T_i} = R/L_{T_e}$ and R/L_n is shown in Figure 6. In the negative R/L_n region the ITG mode turbulence will eventually be stabilized with decreasing R/L_T while for higher R/L_n the TE mode turbulence will instead be excited. As shown in Figure 6c, this leads to a lower background peaking factor with the decrease in R/L_T.

4. Nonlinear results

In order to find the saturation level of the turbulence, nonlinear GENE simulations are needed. Nonlinear simulations are performed for the CBC case ($R/L_{T_e} = R/L_{T_i} = 6.96$) and compared to the EDWM results at $k_y\rho_s = 0.2$ for different values of plasma β. The particle fluxes are shown in Figure 7. The fluid and gyrokinetic particle fluxes agree reasonable well at $\beta = 0\%$ and $\beta = 0.5\%$. For $\beta = 0\%$ the particle flux is negative around $R/L_n = 0$ which means that the particles in a pellet ablation peak would travel inwards. However, at higher β the transport decreases in the negative R/L_n region while it changes sign to outward in the positive region. In this parameter regime the pellet fuelling scheme would be less efficient.

5. Conclusions

In this paper the characteristics of particle transport driven by ITG/TE mode turbulence in regions of hollow density profiles were studied by fluid as well as gyrokinetic simulations, using the EDWM and GENE codes in parameter scans around those of the Cyclone Base Case. In the linear analysis, three main cases were studied, the original Cyclone Base Case with $R/L_{T_e} = R/L_{T_i} = 6.96$ where both the ITG and TE modes were excited, a case with $R/L_{T_i} = 6.96$ and $R/L_{T_e} = 0$ where mainly the ITG mode was driven unstable and a case with $R/L_{T_i} = 0$ and $R/L_{T_e} = 6.96$ which was mainly TE dominated. In the linear gyrokinetic analysis it was found that the ITG mode is dominant in the negative R/L_n region for $k_y\rho_s < 0.5$ and that the TE mode was dominant otherwise in the mixed case with background peaking factor of between $PF \approx 3$ at $k_y\rho_s = 0.2$ to 6 at $k_y\rho_s = 1.2$. In a scan in R/L_n and plasma β, β was found to have a stabilizing effect in the mixed and ITG cases in the negative R/L_n region in both GENE and EDWM. Both models indicated a decrease in background peaking factor with increased plasma β in the mixed case. Increasing magnetic shear also had a stabilizing effect in the negative R/L_n region while adding collisions had a negligible effect. In the nonlinear analysis the particle fluxes are negative around $R/L_n = 0.0$ in the electrostatic case. Adding β effects, however, the inward particle flux in the negative R/L_n region decreases in both models while it changes sign to outwards in the positive gradient region, following the linear results which indicated a decrease in background peaking factor. This may have serious consequences for the efficiency of the pellet fuelling scheme in high β plasmas.

Acknowledgments

The simulations were performed on resources provided by the Swedish National Infrastructure for Computing (SNIC) at the PDC Centre for High Performance Computing (PDC-HPC) and on the HELIOS supercomputer system at the Computational Simulation Centre of International Fusion Energy Research Centre (IFERC-CSC), Aomori, Japan, under the Broader Approach collaboration between Euratom and Japan, implemented by Fusion for Energy and JAEA. This work was funded by a grant from The Swedish Research Council (C0338001).

References

[1] Garzotti L, Figueiredo J, Roach C, Valovič M, Dickinson D, Naylor G, Romanelli M, Scannell R and Szepesi G 2014 *Plasma Physics and Controlled Fusion* **56** 035004
[2] Kotschenreuther M, Rewoldt G and Tang W 1995 *Computer Physics Communications* **88** 128–140
[3] Tegnered D, Nordman H, Oberparleiter M, Strand P, Garzotti L, Lupelli I, Roach C, Romanelli M and Valovic M 2016 Gyrokinetic simulations of transport in pellet fuelled discharges at jet *43rd European Physical Society Conference on Plasma Physics, Leuven, Belgium*
[4] Bourdelle C, Garbet X, Imbeaux F, Casati A, Dubuit N, Guirlet R and Parisot T 2007 *Physics of Plasmas (1994-present)* **14** 112501
[5] Baiocchi B, Bourdelle C, Angioni C, Imbeaux F, Loarte A and Maslov M 2015 *Nuclear Fusion* **55** 123001
[6] http://genecodeorg/
[7] Kadomtsev B and Pogutse O 1971 *Nuclear Fusion* **11** 67
[8] Coppi B and Pegoraro F 1977 *Nuclear Fusion* **17** 969
[9] Horton Jr W, Choi D and Tang W 1981 *Physics of Fluids (1958-1988)* **24** 1077–1085
[10] Guzdar P, Chen L, Tang W and Rutherford P 1983 *Physics of Fluids (1958-1988)* **26** 673–677
[11] Romanelli F 1989 *Physics of Fluids B: Plasma Physics (1989-1993)* **1** 1018–1025
[12] Biglari H, Diamond P and Rosenbluth M 1989 *Physics of Fluids B: Plasma Physics (1989-1993)* **1** 109–118
[13] Dannert T and Jenko F 2005 *Physics of Plasmas (1994-present)* **12** 072309
[14] Dimits A, Bateman G, Beer M, Cohen B, Dorland W, Hammett G, Kim C, Kinsey J, Kotschenreuther M, Kritz A *et al.* 2000 *Physics of Plasmas (1994-present)* **7** 969–983
[15] Weiland J 1999 *Collective Modes in Inhomogeneous Plasmas: Kinetic and Advanced Fluid Theory* (CRC Press)
[16] Strand P, Bateman G, Eriksson A, Houlberg W, Kritz A, Nordman H and Weiland J 2004 Comparisons of anomalous and neoclassical contributions to core particle transport in tokamak discharges *31th EPS Conference, London 2004, European Physical Society* vol 28

[17] Merz F 2008 *Gyrokinetic simulation of multimode plasma turbulence* Ph.D. thesis Universitat Munster
[18] Nordman H, Skyman A, Strand P, Giroud C, Jenko F, Merz F, Naulin V, Tala T, Contributors J E *et al.* 2011 *Plasma Physics and Controlled Fusion* **53** 105005
[19] Pueschel M J, Kammerer M and Jenko F 2008 *Physics of Plasmas* **15** 102310
[20] Jenko F and Dorland W 2001 *Plasma physics and controlled fusion* **43** A141
[21] Skyman A, Tegnered D, Nordman H and Strand P 2014 *Physics of Plasmas (1994-present)* **21** 092305